Applied Water Science (2024) 14:100
https://doi.org/10.1007/s13201-024-02151-0

ORIGINAL ARTICLE

Removal of *Staphylococcus aureus* using electro-fenton, UV/H_2O_2, and combination of electro-fenton and UV/H_2O_2 processes; optimization of operational parameters

Asiyeh Dokhani[1] · Babak kheirkhah[2] · Davood Kalantar-Neyestanaki[3,4] · Farokh Rokhbakhsh-Zamin[1] · Maryam Dolatabadi[5] · Saeid Ahmadzadeh[6]

Received: 22 October 2023 / Accepted: 7 March 2024

Abstract

Staphylococcus aureus (*S. aureus*) is an opportunistic pathogen of the gram-positive variety, known to cause a range of severe infections including cellulitis, pneumonia, osteomyelitis, endocarditis, and sepsis. These infections are associated with significant morbidity and mortality rates in both hospital and community settings. Therefore, it is important to remove *S. aureus* from the aqueous solution. The present study employed response surface methodology as an effective strategy to optimize the removal of *S. aureus* through the electro-Fenton (EF), UV/H_2O_2, and combination EF-UV/H_2O_2 processes. Under the optimized conditions, the maximum removal efficiency in the EF process of 48.5%, UV/H_2O_2 process of 36.2%, and combination EF-UV/H_2O_2 process of 100%. The optimum condition for removal efficiency using combination EF-UV/H_2O_2 process of 100% was attained at *S. aureus* concentration of 5×10^6 CFU mL^{-1}, current density of 8.0 mA cm^{-2}, H_2O_2 dosage of 170 μL L^{-1}, and 2 lamps UV during 7.0 min. Both the production of $^{\bullet}OH$ in the EF and UV/H_2O_2 process and the additive oxidation effect of UV/H_2O_2 are the main reasons for the better performance of combination EF-UV/H_2O_2 process. The results indicate that the EF-UV/H_2O_2 process is highly promising and environmentally sustainable method for treating wastewater samples contaminated with *S. aureus*.

Keywords *Staphylococcus aureus* · Electro-Fenton process · UV/H_2O_2 process · Combination EF-UV/H_2O_2 process · Removal

Introduction

The utilization of recycled wastewater is being contemplated as a strategic remedy in numerous regions or countries facing water scarcity (Yong et al. 2023). Nevertheless, the existence of health risks stemming from biological hazards (such as pathogens) and chemical hazards (like micro-pollutants) in the original water sources, reclaimed wastewater, water used for landscaping, and the final drinking water, poses a growing challenge for public health and the ecological/environmental aspects (Li et al. 2023a; Mgidlana et al. 2023). Bacterial contamination represents a distinct category of water pollution. When pathogens contaminate drinking water, they can lead to infections in the gastrointestinal system, resulting in complications such as diarrhea and cholera. Every year, a significant number of children and elderly individuals lose their lives due to water contaminated with *Escherichia coli* (*E. coli*) and *Staphylococcus aureus* (*S. aureus*), two bacteria that have developed resistance to commonly used antimicrobial agents

✉ Saeid Ahmadzadeh
chem_ahmadzadeh@yahoo.com;
saeid.ahmadzadeh@kmu.ac.ir

[1] Department of Microbiology, Faculty of Science, Kerman Branch, Islamic Azad University, Kerman, Iran

[2] Department of Microbiology, Veterinary Medicine Faculty, Baft Branch, Islamic Azad University, Baft, Iran

[3] Medical Mycology and Bacteriology Research Center, Kerman University of Medical Sciences, Kerman, Iran

[4] Department of Medical Microbiology (Bacteriology and Virology), Afzalipour Faculty of Medicine, Kerman University of Medical Sciences, Kerman, Iran

[5] Environmental Health Engineering Research Center, Kerman University of Medical Sciences, Kerman, Iran

[6] Pharmaceutics Research Center, Institute of Neuropharmacology, Kerman University of Medical Sciences, Kerman, Iran

(Ausbacher et al. 2023). *S. aureus*, a type of Gram-positive bacterium, is widely recognized as a prominent pathogen associated with severe cases of foodborne and waterborn diseases and has consistently posed a significant challenge in various human infections, especially due to its resistance to antibiotics (Wan Omar et al. 2023; Zhang et al. 2023).

These concerns pose a significant challenge for public health and environmental aspects. Therefore controlling the presence of pathogenic bacteria in water is crucial to avoid potential health risks related to water contamination (Aziz et al. 2013; Iqbal et al. 2019). Disinfection is the final step in wastewater treatment plants aimed at reducing the presence of pathogenic bacteria. Nonetheless, pathogenic bacteria can evade the disinfection processes and consequently be present in treated wastewater, ultimately entering the aquatic environment (Yang et al. 2023; Abbas et al. 2018). This poses a significant concern for human health since treated wastewater, depending on its subsequent utilization, can serve as a potential source of waterborne diseases (Sabatino et al. 2022; Kousar et al. 2022). Traditional water treatment methods have proven to be ineffective in preventing and eliminating pathogenic microorganisms from water (Bokhari et al. 2022). Consequently, there is a pressing need for innovative materials that possess antimicrobial properties in order to enhance the quality of contaminated water (Mphuthi et al. 2023; Liu et al. 2023).

Advanced oxidation processes (AOPs), which operate at or near ambient temperature, include Fenton, photo-Fenton, electro-Fenton, UV-based processes, and photocatalytic redox processes. These methods are specifically employed for water and wastewater treatment. The main objective of AOPs is to generate highly reactive free radicals (Mansour et al. 2023; Babu Ponnusami et al. 2023). Hydroxyl radicals ($^{\bullet}OH$) are extremely effective in the destruction of organic molecules due to their high standard potential (E = 2.8 vs. SHE, or "Standard Hydrogen electrode "), as well as their react quickly and non-selective (Jiang et al. 2022; Thakur et al. 2023).

The Fenton reaction, being a typical of AOPs, effectively oxidizes organic pollutants by utilizing $^{\bullet}OH$ generated from the reaction between H_2O_2 and Fe^{2+}. In the typical procedure, the Fenton reaction operates through a cyclic reaction involving H_2O_2. As represented in reaction (1) and (2), under acidic conditions reaction (1), Fe^{2+} initially reacts with H_2O_2 to produce $^{\bullet}OH$ and Fe^{3+}. Following this, the generated Fe^{3+} reacts with H_2O_2 to form H_2O_2 radicals and regenerate Fe^{2+} reaction. (2) (Qi et al. 2023; Dai et al. 2023).

$$Fe^{2+} + H_2O_2 \rightarrow Fe^{3+} + HO^{\cdot} + OH^{-} \tag{1}$$

$$Fe^{3+} + H_2O_2 \rightarrow Fe^{2+} + HO_2^{\cdot} + H^{+} \tag{2}$$

However, traditional Fenton technology suffers from certain drawbacks such as the need for chemical dosing, generation of substantial sludge, lengthy treatment duration, and difficulties in control, which restrict its widespread implementation. Additionally, the pH tolerance range of the conventional Fenton process is limited, as it can only operate efficiently under acidic conditions.

The electro-Fenton (EF) process has gained significant attention due to its numerous advantages, including high efficiency, minimal land usage, user-friendly operation, and environmental friendliness. This process addresses several drawbacks of the conventional Fenton process, such as mitigating the risks associated with the storage and transportation of Ferric sulfate, as well as reducing the formation of excessive iron sludge (Li et al. 2023b). UV-based AOPs represent a promising category of advanced treatment technologies that have been developed with the aim of eliminating pollutants and enhancing the quality of treated water and wastewater. UV-AOPs employ a collaborative approach involving UV light, chemical oxidants (such as H_2O_2, persulfate, and chlorine), or photocatalysts to efficiently oxidize pollutants (Wang et al. 2018). UV irradiation combined with H_2O_2 has garnered significant attention from environmentalists among various AOPs due to its remarkable ability to effectively eliminate pollutants present in treated effluents (Salim et al. 2022). Enhanced Fenton-based and UV processes, including the innovative photoelectro-Fenton (PEF) process, have emerged to minimize or even eliminate sludge production. These advanced methods are specifically engineered to operate efficiently at elevated pH levels, even under near-neutral conditions (Brillas 2022; Arshad et al. 2020).

This research focuses on the removal of *S. aureus* investigation and optimization of various parameters in the EF process, with the aim of studying. Initially, key factors such as the initial concentration of *S. aureus*, current density, and H_2O_2 dosage are investigated using response surface methodology (RSM). Subsequently, the removal of *S. aureus* is analyzed by employing the UV/H_2O_2 process. Finally, the removal process is thoroughly examined and optimized through the application of the PEF process.

Experimental and methods

Chemicals

Analytical grade sodium hydroxide (NaOH, purity: ≥ 98.0%), Hydrochloric acid (HCl, purity: 37.0%), sodium sulfate (Na_2SO_4, purity: ≥ 99.0%), acetone (C_3H_6O, purity: ≥ 99.0%), potassium chloride (KCl, purity: ≥ 99.0%), hydrogen peroxide (H_2O_2, purity: 30.0%), chloroform ($CHCl_3$, purity: ≥ 99.0%), isoamyl alcohol ($(CH_3)_2CHCH_2CH_2OH$, purity: ≥ 95.0%), ethanol (C_2H_6O, purity: ≥ 70%.), isopropyl alcohol (C_3H_8O, purity: ≥ 99.5%), lactose, glucose, and sucrose were prepared from Merck® company. Moreover, safranin, triple sugar iron agar, MacConkey agar, trypticase soy agar with 5% sheep blood, plate count agar was prepared from Merck company.

Electrochemical reactor

The EF experiments were carried out under batch conditions using an electrochemical reactor. An iron plate with 99.5% purity and dimensions of 60 × 6 × 1 mm was utilized as both the anode and cathode electrodes, which were positioned vertically and parallel to each other. The electrodes were of the same size, with a constant inter-distance of 3.0 cm within the electrochemical reactor. The reaction time and pH were kept constant at 15 min and 6.5, respectively, throughout the EF process. The removal efficiency of *S. aureus* and the electrical energy consumption (EEC) of the process were determined using Eq. (3) and (4), respectively.

$$\%\text{Removal} = \frac{C_{(S.Aureus-0)} - C_{(S.Aureus-t)}}{C_{(SA-0)}} \times 100 \tag{3}$$

where $C_{S.aureus\text{-}0}$ and $C_{S.aureus\text{-}t}$ (CFU mL^{-1}) denote the *S. aureus* concentration before EF process and time t, respectively.

$$\text{EEC} = \left(\frac{UIt}{V}\right) \tag{4}$$

where U, I, t, and V are applied voltage (U), applied electrical current (A), reaction time (h) and volume of sample (L), respectively.

The UV/H_2O_2 process was conducted by introducing synthetic wastewater and H_2O_2 into a 250 ml UV/H_2O_2 reactor in UV cabinet. To ensure the temperature and radiation output of the lamps were balanced, a period of 30 min was allocated before each experimental run for the lamps (consisting of 1 to 3 lamps) to be switched on and reach equilibrium.

Previous experiments have demonstrated that a period of continuous exposure to radiation lasting 10 min is adequate to achieve a state of equilibrium. Therefore, for the purpose of this experiment, a fixed reaction time of 10 min was established. After each sampling in EF, UV/H_2O_2, and PEF, the samples were promptly quenched by adding $Na_2S_2O_3$. This addition serves to eliminate any excess H_2O_2 and halt the reaction. To minimize errors, performed three repetitions of all experiments and presented the average value for each run.

Statistical analysis and modeling using RSM

Response Surface Methodology (RSM) was utilized to develop a statistical model that evaluates and optimizes the impact of operating parameters as independent variables on the removal efficiency of the EF process, which serves as the response variable. For the current study, three independent variables were chosen as A: *S. aureus* concentration (X_1), B: current density (X_2), C: H_2O_2 dosage (X_3). The effect of variables was investigated at five different coded levels of −α, −1, 0, +1, and +α, in which the number of α is equal to 1.68. The *S. aureus* removal efficiency was selected as response. Table 1 summarizes the actual and coded values of the variables.

The obtained data from the experiments were analyzed using Design Expert 11.0 software. The analysis of variance (ANOVA) was investigated. The results obtained indicated that the experimental data showed the highest level of agreement with the second-order polynomial model presented below (Eq. (5)) (Wang et al. 2022):

$$Y = \beta_0 + \sum_{i=1}^{n} \beta_i X_i + \sum_{i=1}^{n} \beta_{ii} X_i^2 + \sum_{i=1}^{n-1} \sum_{j=i+1}^{n} \beta_{ij} X_i X_j + \varepsilon \tag{5}$$

where Y, X_i, and X_j denote the predicted response and the input variables of i and j, respectively. Moreover, the parameters β_0, β_i, β_{ii}, and β_{ij} denote the regression constants for intercept, linear, quadratic, and interaction coefficients, respectively. Also, ε and n denote the error, and the number of variables studied. The experiments were conducted in a random manner, and the designed experiments along with the corresponding values of the model responses are presented in Table 2.

Results and discussion

Statistical analysis and model fitting

To evaluate the appropriateness and significance of the constructed model, we conducted an ANOVA, utilizing the

Table 1 Experimental main operating parameter and their levels in CCD

Coded Variables (X_i)	Factors (U_i)	Unite	Experimental Field				
			−α	−1 level	0	+1 level	+α
X_1	A: *S. aureus* concentration	(CFU mL^{-1})	1×10^4	2×10^6	5×10^6	8×10^6	10×10^6
X_3	B: Current density	(mA cm^{-2})	3.0	4.8	7.5	10	12
X_2	C: H_2O_2 dosage	(μL L^{-1})	20	56	110	163	200

Table 2 Experimental design for the influences of the three independent variables on the *S. aureus* removal efficiency in coded values and experimental results

Run	actual value			coded value			*S. aureus* Removal Efficiency (%)
	A ($CFU\ mL^{-1}$)	B ($mA\ cm^{-2}$)	C ($\mu L\ L^{-1}$)	X_1	X_2	X_3	
1	5×10^6	7.5	20.0	0	0	−1.68	22.2
2	5×10^6	7.5	110	0	0	0	38.5
3	5×10^6	7.5	110	0	0	0	38.9
4	5×10^6	3.0	110	0	−1.68	0	32.6
5	8×10^6	10.2	164	+1	+1	+1	40.6
6	5×10^6	7.5	110	0	0	0	38.8
7	5×10^6	7.5	200	0	0	+1.68	39.8
8	2×10^6	10.2	57	−1	+1	−1	38.0
9	8×10^6	10.2	57	+1	+1	−1	29.5
10	5×10^6	12.0	110	0	+1.68	0	45.7
11	8×10^6	4.8	164	+1	−1	+1	34.9
12	2×10^6	10.2	164	−1	+1	+1	48.8
13	5×10^6	7.5	110	0	0	0	38.1
14	2×10^6	4.8	164	−1	−1	+1	44.3
15	2×10^6	4.8	57	−1	−1	−1	32.9
16	5×10^6	7.5	110	0	0	0	38.0
17	10×10^6	7.5	110	+1.68	0	0	31.7
18	5×10^6	7.5	110	0	0	0	37.2
19	8×10^6	4.8	57	+1	−1	−1	25.2
20	1×10^6	7.5	110	−1.68	0	0	47.1

statistical indicators of *F* value and *p* value. The findings from this analysis are presented in Table 3.

Table 3 shows that the developed model achieved an *F* value of 209.5 for the removal efficiency of *S. aureus*. Additionally, the *p* values associated with the developed model was found to be less than 0.0001. Therefore, it can be concluded that the fitted model was statistically significant (p value < 0.05) at a 95% confidence level (CI).

The removal efficiency of *S. aureus*, as influenced by the independent variables, is represented by the coded form in Eq. (6), which illustrates the relationship between the independent variables and response.

$$\text{removal efficiency}(\%) = 38.88 - 4.37X_1 + 3.04X_2 + 5.32X_3 - 2.56X_3^2 \tag{6}$$

X_1, X_2, and X_3 are the code values of *S. aureus* concentration, current density, and the H_2O_2 dosage, respectively. Moreover, $X_3{}^2$ is the quadratics effects of H_2O_2 dosage. The presence of negative or positive signs associated with the terms in the equation signifies the respective synergistic and antagonistic effects of each factor on the removal efficiency of *S. aureus* in the EF process, which serves as the dependent variable. The quadratic model proposed for the removal

Table 3 Analysis of variance for the response surface quadratic model

Source	Sum of Squares	Degree of freedom (df)	Mean Squares	*F*-value	Probability *p* value > *F*
Model	870.3	4	217.6	209.5	< 0.0001
X_1	260.9	1	260.9	251.1	< 0.0001
X_2	126.5	1	126.5	121.9	< 0.0001
X_3	386.6	1	386.6	372.2	< 0.0001
X_3^2	96.3	1	96.6	92.7	< 0.0001
Residual	15.6	15	1.0	–	–
Lack of Fit	13.6	10	1.4	3.53	0.0881
Pure Error	1.9	5	0.4	–	–
Cor. Total	885.8	19	–	–	–
$R^2 = 0.9824$	Adj.$R^2 = 0.9777$	Pred.$R^2 = 0.9663$	AP = 51.7		

efficiency of *S. aureus* demonstrated that the developed regression model was the most suitable fit for the examined parameters.

The coefficient of determination (R^2) for the removal efficiencies, as predicted by the developed model (*S. aureus* removal efficiency), was 0.9824. This value indicates the extent to which the expected and observed values of removal efficiency align with each other. The proposed model achieved an adjusted R^2 (Adj.R^2) value of 0.9777 for the removal efficiency. Additionally, the predicted R^2 (Pred.R^2) value was determined to be 0.9663.

Based on the discrepancy between Adj.R^2 and Pred.R^2 being below 0.20, it can be concluded that the developed model accurately predicts the removal efficiency of the proposed EF process. Additionally, this prediction demonstrates a significant level of agreement with the actual values, indicating a high level of satisfaction. The adequate precision (AP) value, expressed as the signal-to-noise ratio, achieved a value of 51.7 for the *S. aureus* removal efficiency. As the obtained value exceed 4, it is confirmed that the proposed model effectively explores the design space with great precision and dependability. The calculated *p*-value of 0.0881, indicating the lack of fit in the proposed regression model for removal efficiency, exceeds the significance level of 0.05. This suggests that the relationship between the input variables and the model response is deemed appropriate, affirming the significance of the developed model.

Diagnostic diagrams were plotted in order to assess the normal distribution and adequacy of the data, as demonstrated in Fig. 1.

Based on Fig. 1a, it is clear that there is a satisfactory agreement between the predicted values and the experimentally obtained values for the *S. aureus* removal efficiency of the proposed model. This agreement confirms the competence of the model in accurately predicting the response values. Furthermore, the normal distribution of the model, as depicted in Fig. 1b, indicates that the externally observed residual points align closely along a nearly straight line.

Pareto analysis

The Pareto analysis was performed in order to examine the influential factors' contribution to the response variable for the predicted model. To evaluate the significance of operating parameters on the *S. aureus* efficiency removal, Pareto analysis was conducted. The result, presented in Fig. 2, clearly demonstrate the operating parameter with the most substantial influence on the response. As can be seen, the impact of H_2O_2 dosage and the initial concentration of *S. aureus* on the removal efficiency are evident. Furthermore, the quadratic effect of H_2O_2 dosage (X_3^2) influenced the removal efficiency.

Effect of parameters

Effect of *S. aurous* initial concentration

The effect of *S. aureus* initial concentration on the removal efficiency using the EF process was investigated at various concentrations ranging from 1×10^4–10×10^6 CFU mL^{-1}. The simultaneous effect of current density and initial *S. aureus* concentrations on the removal efficiency using EF process were investigated and displayed in the contour plot of Fig. 3.

The observation revealed a decrease in removal efficiency as the initial concentration of *S. aureus* increased

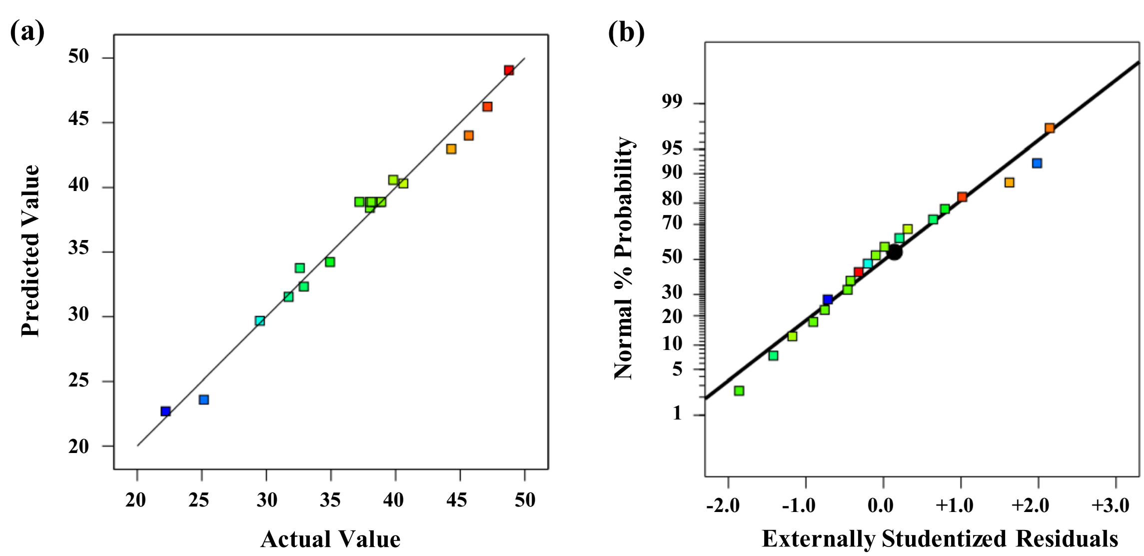

Fig. 1 Diagnostic diagrams **a** plot of the predicted values *vs.* the actual values, **b** normal probability plot of externally studentized residuals

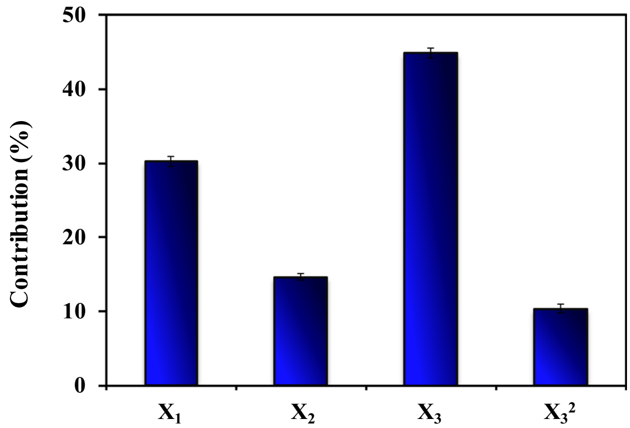

Fig. 2 Contribution of significant parameters on the *S. aureus* removal efficiency using EF process

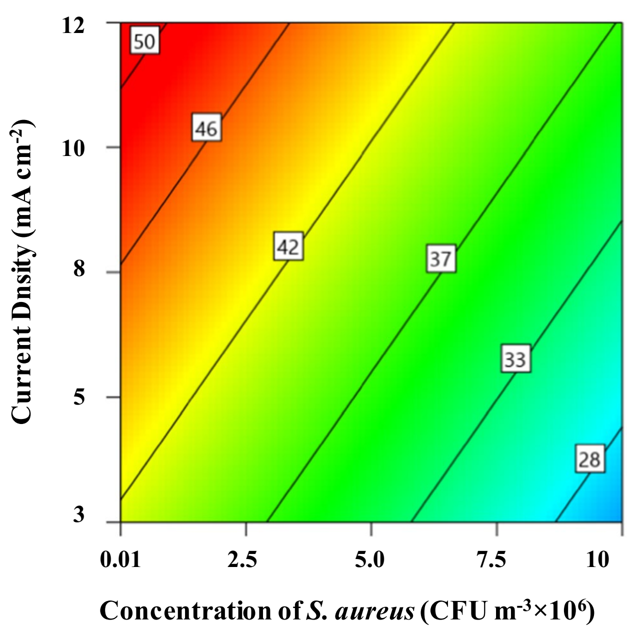

Fig. 3 Contour plot of the combined effect of current density and initial *S. aureus* concentrations on the *S. aureus* removal efficiency

under constant conditions, including a current density of 7.5 mA cm^{-2}, H_2O_2 dosage of 110 μL L^{-1}, reaction time of 15 min, and pH of 6.5. Specifically, the removal efficiency of *S. aureus* decreased from 46.2% to 31.5% when the initial concentration increased from 1×10^4 to 10×10^6 CFU mL^{-1}.

It is important to note that under constant conditions, the generation of $^{\bullet}OH$ remains consistent. However, as the *S. aureus* concentration increases to higher levels, the proportion of $^{\bullet}OH$ compared to the *S. aureus* count decreases. The decrease in the proportion of hydroxyl radicals ($^{\bullet}OH$) subsequently leads to a reduction in the efficiency of removing *S. aureus*.

Effect of current density

Effect of the current density on *S. aureus* removal efficiency was investigated in the range of 3–12 mA m^{-2} during reaction time of 15 min, *S. aureus* concentration of 5×10^6 CFU mL^{-1}, and pH of 6.5. The obtained experimental results were illustrated by contour plot in Fig. 3.

It was observed that the *S. aureus* removal efficiency is increased with increasing the current density. The removal efficiency of *S. aureus* was increased from 33.8% to 44.5% when the current density increased from 3 to 12 mA cm^{-2}. It is evident that the use of a higher current density to the electrochemical reactor leads to an increase in the rate of Fe^{+2} ion generations, as indicated by reaction (7). The acquired response ascribed to the accelerating of Fe^{2+} ion generation, which resulted in the progression of Fenton reaction and generation of more $^{\bullet}OH$ (Amarzadeh et al. 2023; Javed et al. 2021).

$$Fe_{(s)} \rightarrow Fe^{2+}_{(aq)} + 2e^{-} \tag{7}$$

Effect of H_2O_2 dosage

According to literature surveys, the removal efficiency is significantly influenced by the dosage of H_2O_2 used as an oxidizing agent in EF process. Therefore, the present study conducted a thorough investigation to identify the optimal dosage of H_2O_2 within the range of 20–200 μL L^{-1}. Effect of H_2O_2 dosage for *S. aureus* removal efficiency was investigated under center point conditions, including a current density of 7.5 mA m^{-2}, *S. aureus* concentration of 5×10^6 CFU mL^{-1}, pH of 6.5, and a reaction time of 15 min during the EF process. The results obtained are depicted in Fig. 4.

The removal efficiency of *S. aureus* was increased from 22.7% to 42.6% when the H_2O_2 dosage increased from 20 to 170 μL L^{-1}. The increase in removal efficiency observed when the dosage of H_2O_2 was increasing from 20 to 170 μL L^{-1} can be attributed to the acceleration of the Fenton reaction and the generation of a greater amount of $^{\bullet}OH$ (reactions 5 and 6). However, when the dosage of H_2O_2 exceeds 170 μL L^{-1}, the removal efficiency of *S. aureus* was decreases.

Similar studies have attributed the reason for this phenomenon to the following reactions, as demonstrated in side reactions (reactions 10–2), the observed phenomenon may be attributed to an excessive quantity of H_2O_2 ranging from 170 to 200 μL L^{-1}, leading to the consuming of free $^{\bullet}OH$. $HO_2^{\bullet}$, acting as a weak oxidizing agent, deactivates the hydroxyl radicals, as described. Furthermore, in high dosage of H_2O_2, the interaction between $^{\bullet}OH$ intensifies, leading to

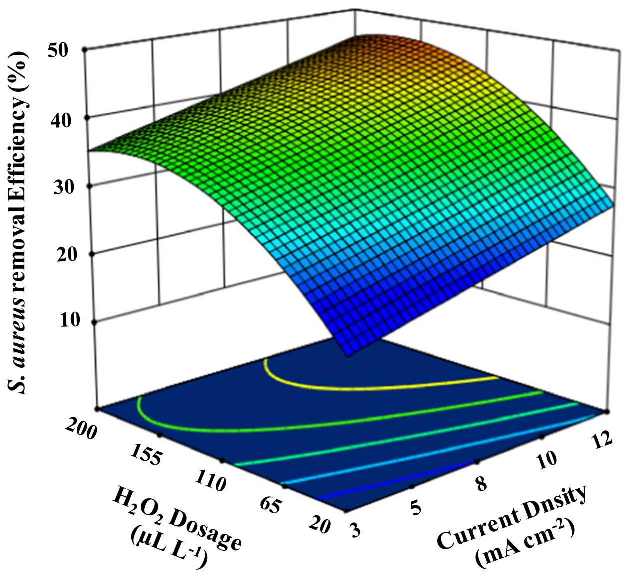

Fig. 4 3D surface plot of the combined effect of H_2O_2 dosage and current density on the *S. aureus* removal efficiency

a greater depletion of oxidizing agents used for the removal efficiency (Iqbal et al. 2023; Rahman et al. 2023).

$$H_2O_2 + h\upsilon \rightarrow 2HO^{\cdot} \quad (8)$$

$$H_2O_2 + h\upsilon \rightarrow H^{\cdot} + HO^{\cdot} \quad (9)$$

$$H_2O_2 + HO^{\cdot} \rightarrow HO_2^{\cdot} + H_2O \quad (10)$$

$$HO_2^{\cdot} + HO^{\cdot} \rightarrow H_2O + O_2 \quad (11)$$

$$HO^{\cdot} + HO^{\cdot} \rightarrow H_2O_2 \quad (12)$$

Optimal operating condition for EF process

The optimization of analytical procedures has garnered significant attention with the use of RSM in comparison to the classical approach known as One factor at a time (OFAT). This is primarily because RSM has the ability to yield valuable information with a limited number of designed experiments. In order to attain the highest efficiency in removing *S. aureus* (response), the optimization of operating conditions was carried out to identify the optimal values for these parameters. The process of optimization involved the utilization of a numerical technique integrated within the Design-Expert software. The variables were set with the objective of achieving values within a specified range, while the primary focus was placed on maximizing *S. aureus* removal efficiency. Based on the outcome findings it was found that the best *S. aureus* removal efficiency of 48.5% was achieved at *S. aureus* concentration of 5×10^6 CFU mL^{-1}, H_2O_2 dosage amount of 170 μL L^{-1}, pH 6.5, reaction time 15 min and current density 8.0 mA.cm^{-2}.

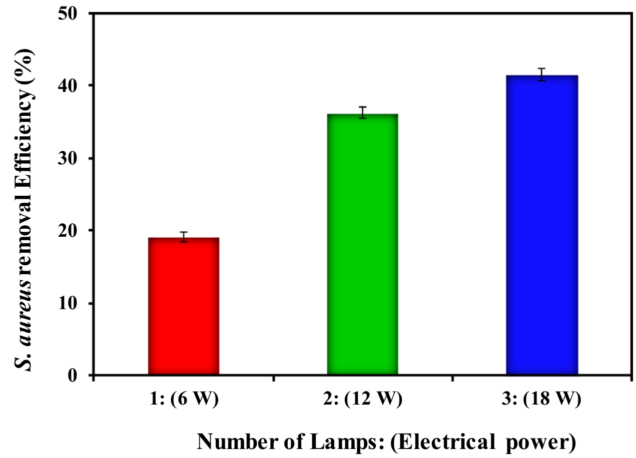

Fig. 5 Effect of number of lamps UV on removal efficiency of *S. aureus* throughout UV/H_2O_2 process

UV/H_2O_2 process

The optimization of light intensity emitted by 1 to 3 UV lamps was investigated during the UV/H_2O_2 process under the following conditions: *S. aureus* concentration of 5×10^6 CFU mL^{-1}, H_2O_2 dosage of 170 μL L^{-1}, and pH 6.5. These conditions were selected based on the optimized values in the EF process. Samples were manually collected at reaction time 0 and 10 min of each experiment. The results obtained are depicted in the Fig. 5.

The results showed that the removal efficiencies increased from 19.1%, 36.2%, and 41.4% by increasing the number of lamps: (Electrical power) from 1 lamp (6 W), 2 lamps (12 W), and 3 lamps (18 W). On the other hand, increasing the number lamps from 1 to 3 lamps increased the electrical energy consumption during UV/H_2O_2 process. Increased levels of *S. aureus* removal efficiency was observed as the intensity of radiation escalated, primarily attributed to the generation of $^{\bullet}OH$ via the photolysis of the oxidant (Vitale et al. 2023; Bhatti et al. 2020).

de Souza et al. and Srithep et al. reported in her study that the UV radiation in wavelength of 254 nm breaks the chemical bond of –O–O– in H_2O_2 and creates $^{\bullet}OH$, according to reaction (5) (de Souza et al. 2023; Srithep et al. 2017; Bokhari et al. 2020). The generation of $^{\bullet}OH$ enhances the effectiveness of the removal process (Zhu et al. 2023). Based on the obtained results, the removal efficiency of using 2 lamps (36.2%) is very close to that of using 3 lamps (41.5%). Therefore, 2 lamps (12 W), is selected as the optimal conditions.

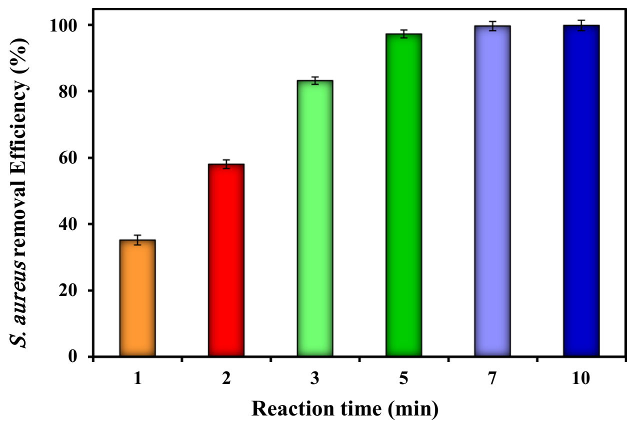

Fig. 6 Effect of *S. aureus* removal using combination of EF and UV/H_2O_2 process

Combination EF- UV/H_2O_2 process

The combined effect of the EF and UV/H_2O_2 processes was investigated under the specified conditions: a concentration of *S. aureus* at 5×10^6 CFU mL^{-1}, dosage of 170 µL L^{-1} of H_2O_2, pH of 6.5, current density of 8.0 mA cm^{-2}, and 2 lamps UV. These conditions were chosen based on optimized values in the EF and UV/H_2O_2 process. The samples were conducted at reaction times ranging from 1 to 10 min for each experiment. Figure 6 illustrates the results obtained.

The results clearly indicate that the removal efficiencies of *S. aureus* increased with the extension of reaction time. Specifically, the removal efficiencies improved from 35.2%, 58.1%, 83.3%, 97.4%, 99.8%, to 100% when the reaction time was increased to 1, 2, 3, 5, 7, and 10 min, respectively. According to obtained result, the combination of EF and UV/H_2O_2 process was more efficient for *S. aureus* removal efficiency than EF and UV/H_2O_2 alone. The increase in removal efficiency may be attributed to the enhancement of the Fenton reaction rate through simultaneous UV irradiation. This phenomenon assists in the regeneration of the required Fe^{2+} species (reaction 13).

$$Fe^{3+} + h\upsilon \rightarrow Fe^{2+} + HO^{\cdot} \qquad (13)$$

The obtained results show that the coupling of EF process with UV/H_2O_2 process can be a promising approach for the removal of *S. aureus*.

Conclusions

In this study, substantial efforts were undertaken to remove S. aureus from contaminated water. The present research aimed to optimize the operational parameters of the EF, UV/H_2O_2, and combination processes using response surface methodology (RSM) based on central composite design (CCD). These measures were implemented to improve the efficacy of *S. aureus* removal. According to our findings, the combination of the EF and UV/H_2O_2 process was more efficient for removal efficiency than EF process (48.5%) and UV/H_2O_2 process (36.2%) alone. Furthermore, the analysis of variance showed the adequacy of the correspondence of the experimental data to the theoretically determined ones, i.e., the obtained mathematical model. The significant improvement of removal efficiency in combination of the EF and UV/H_2O_2 process highlighted the synergistic effect between EF and UV/H_2O_2 process. The results show that $^{\bullet}$OH was the main oxidant species contributed in removal efficiency of *S. aureus* under the EF and UV/H_2O_2, and combination process. The findings indicate that the combination EF and UV/H_2O_2 has significant potential as a highly efficient and environmentally friendly method for the removal of *S. aureus*.

Acknowledgements The authors would like to express their appreciation to Kerman University of Medical Sciences [Grant Number 402000584] for supporting the current work.

Funding This work received a grant from the Kerman University of Medical Sciences [Grant Number 402000584].

Declarations

Conflict of interest The authors declare that they have no conflict of interest regarding the publication of the current paper.

Ethical approval The Ethics Committee of Kerman University of Medical Sciences approved the study (IR.KMU.REC.1402.584).

References

Abbas M et al (2018) Vibrio fischeri bioluminescence inhibition assay for ecotoxicity assessment: a review. Sci Total Environ 626:1295–1309

Amarzadeh M et al (2023) Heterogeneous fenton-like photocatalytic process towards the eradication of tetracycline under UV irradiation: mechanism elucidation and environmental risk analysis. Water 15(13):2336

Arshad R et al (2020) Degradation product distribution of Reactive Red-147 dye treated by $UV/H_2O_2/TiO_2$ advanced oxidation process. J Market Res 9(3):3168–3178
Ausbacher D et al (2023) α, α-disubstituted β-amino amides eliminate Staphylococcus aureus biofilms by membrane disruption and biomass removal. Biofilm 6:100151
Aziz HA et al (2013) The performance of Electro-Fenton oxidation in the removal of coliform bacteria from landfill leachate. Waste Manage 33(2):396–400
Babu Ponnusami A et al (2023) Advanced oxidation process (AOP) combined biological process for wastewater treatment: a review on advancements, feasibility and practicability of combined techniques. Environ Res 237:116944
Bhatti HN et al (2020) Facile synthesis of zero valent iron and photocatalytic application for the degradation of dyes. Mater Res Express 7(1):015802
Bokhari TH et al (2020) UV/H_2O_2, $UV/H_2O_2/SnO_2$ and Fe/H2O2 based advanced oxidation processes for the degradation of disperse violet 63 in aqueous medium. Mater Res Express 7(1):015531
Bokhari TH et al (2022) Degradation of a pigment red 238 using UV, UV/H_2O_2, $UV/H_2O_2/SnO_2$ and fenton processes. Pol J Environ Stud 31(1):619–623
Brillas E (2022) Fenton, photo-Fenton, electro-Fenton, and their combined treatments for the removal of insecticides from waters and soils. Rev Sep Purif Technol 284:120290
Dai C et al (2023) Recent progress in modification and composite strategies of graphitic carbon nitride as catalysts for heterogeneous photo-Fenton reaction. Mater Sci Semicond Process 167:107807
de Souza AB et al (2023) Removal of miconazole from water by O_3, UV/H_2O_2 and electrochemical advanced oxidation: real-time process monitoring and degradation pathway elucidation. J Environ Chem Eng 11(3):109993
Iqbal M et al (2019) Bioassays based on higher plants as excellent dosimeters for ecotoxicity monitoring: a review. Chem Int 5(1):1–80
Iqbal Z et al (2023) Photocatalytic degradation of dyes in aqueous media by gum shellac stabilized selenium nanoparticles. Z Phys Chem 237(8):1139–1152
Javed M et al (2021) Photosynthetic acclamatory response of Panicum antidotale Retz. populations to root zone desiccation stress. Braz J Biol 84:e252735
Jiang Y et al (2022) Recent progress in Fenton/Fenton-like reactions for the removal of antibiotics in aqueous environments. Ecotoxicol Environ Saf 236:113464
Kousar T et al (2022) $SnO_2/UV/H_2O_2$ and $TiO_2/UV/H_2O_2$ efficiency for the degradation of reactive yellow 160a: by-product distribution. Cytotox Mutagenicity Eval Catal 12(5):553
Li F et al (2023a) Efficient photo-Fenton reaction for tetracycline and antibiotic resistant bacteria removal using hollow Fe-doped In_2O_3 nanotubes: from theoretical research to practical application. Water Res 240:120088
Li X et al (2023b) Carbonaceous materials applied for cathode electro-Fenton technology on the emerging contaminants degradation. Process Saf Environ Prot 169:186–198
Liu S et al (2023) The potential risks posed by micro-nanoplastics to the safety of disinfected drinking water. J Hazard Mater 450:131089
Mansour MS et al (2023) Removal of Eosin Yellow dye from industrial wastewater using UV/H_2O_2 and photoelectro-Fenton techniques. J Photochem Photobiol A 436:114411
Mgidlana S et al (2023) Dual action of asymmetrical zinc(II) phthalocyanines conjugated to silver tungstate nanoparticles towards photodegradation of tetracycline and inactivation of Staphylococcus aureus bacteria. J Photochem Photobiol A 437:114444
Mphuthi BR et al (2023) Hemp seed nanoparticle composites for removing lead, methylene blue, and ibuprofen from an aqueous solution and their antimicrobial towards Escherichia coli and Staphylococcus aureus. Case Stud Chem Environ Eng 8:100436
Qi J et al (2023) Nanomaterials-modulated Fenton reactions: strategies, chemodynamic therapy and future trends. Chem Eng J 466:142960
Rahman TU et al (2023) Progress in plasma-based doping semiconductor photocatalysts for efficient pollutant remediation and hydrogen generation. Sep Purif Technol 24:124141
Sabatino R et al (2022) The ZVI-Fenton process affects the total load of human pathogenic bacteria in wastewater samples. J Water Process Eng 47:102668
Salim NAA et al (2022) A two-stage batch system for phosphate removal from wastewater by iron-coated waste mussel shell to assess the optimum adsorbent dosage. J Water Chem Technol 44(1):10–20
Srithep S et al (2017) Kinetic removal of haloacetonitrile precursors by photo-based advanced oxidation processes (UV/H_2O_2, UV/O_3, and $UV/H_2O_2/O_3$). Chemosphere 176:25–31
Thakur AK et al (2023) Pharmaceutical waste-water treatment via advanced oxidation based integrated processes: an engineering and economic perspective. J Water Process Eng 54:103977
Vitale P et al (2023) Degradation of printing ink effluent and industrial predesign by UV/H2O2 treatment: a kinetic study. Clean Waste Syst 5:100106
Wan Omar WH et al (2023) Effect of natural antibacterial clays against single biofilm formation by Staphylococcus aureus and Salmonella Typhimurium bacteria on a stainless-steel surface. Int J Food Microbiol 394:110184
Wang W-L et al (2018) Potential risks from UV/H2O2 oxidation and UV photocatalysis: a review of toxic, assimilable, and sensory-unpleasant transformation products. Water Res 141:109–125
Wang L et al (2022) Metal-organic frameworks-derived catalysts for contaminant degradation in persulfate-based advanced oxidation processes. J Clean Prod 375:134118
Yang H et al (2023) Magnetic photocatalytic antimicrobial materials for water disinfection. Sep Purif Technol 325:124697
Yong S-S et al (2023) Bacterial composition of refrigerators in households and inactivation of airborne Staphylococcus aureus using a TiO_2-UVLED module in a 512 L aerobiology chamber. Food Microbiol 114:104274
Zhang B et al (2023) Antibacterial activity and mechanism of slightly acidic electrolyzed water (SAEW) combined with ultraviolet light against Staphylococcus aureus. LWT 182:114746
Zhu B et al (2023) Insights into the mechanisms underlying the degradation of xylooligosaccharides in UV/H_2O_2 system. Carbohyd Polym 317:121091